ELSEVIER

Artificial Intelligence in Medicine 571 (2000) 1–24

Artificial Intelligence in Medicine

www.elsevier.com/locate/artmed

Fuzzy methods in tremor assessment, prediction, and rehabilitation

Horia-Nicolai L. Teodorescu[a,*,1], Mircea Chelaru[b], Abraham Kandel[a], Ioan Tofan[c], Mihaela Irimia[c]

[a]*Computer Science and Engineering (CSEE), University of South Florida, 4202 E. Fowler Avenue, Tampa, FL 33620, USA*

[b]*Department of Psychology: Experimental, Duke University, Box 90086, Durham, NC 27708-0086, USA*

[c]*Department of Psychiatry, Policlinic MI, Ferdinand Blvd., Bucharest, Romania*

Received 20 April 2000; received in revised form 26 June 2000; accepted 1 August 2000

Abstract

Tremor is a disabling condition for a large segment of population, mainly elderly. To the present date, there are no adequate tools to diagnose and help rehabilitation of subjects with tremor, but recently there is a tremendous surge of interest in the research in the field. We report on the use of fuzzy methods in applications for rehabilitation, namely in tremor diagnosing and control. We synthesize our results regarding the characterization of the tremor by means of nonlinear dynamics techniques and fuzzy logic, and the prediction of tremor movements in view of rehabilitation purposes. Based on linear and nonlinear analysis of tremor, and using fuzzy aggregation, the fusing of tremor parameters in global functional disabling factors is proposed. Nonlinear dynamic parameters, namely correlation dimension and Lyapunov exponent is used in order to improve the assessment of tremor. The benefits of the fuzzy fused tremor parameters rely on more complete and accurate assessment of the functional impairment and on improved feedback for rehabilitation, based on the fused parameters of the tremor. Further steps in rehabilitation may require external muscular control. In turn, the control of tremor by electrical stimulation requires movement prediction. Several neural and neuro-fuzzy predictors are compared and a neuro-fuzzy predictor is presented, allowing us five-step ahead prediction, with an RMS error of the order of 10%. The benefits of the neuro-fuzzy predictor are good prediction capability, versatility, and apparently a high robustness to individual variations of the tremor. The reported research, which extended over several years and included development of sensors, equipment, and software, has been aimed to development of products. The results may also open new ways in tremor rehabilitation.

Keywords: Rehabilitation; Tremor; Movement analysis; Measurement system; Nonlinear dynamics; Fuzzy data fusing; Neuro-fuzzy predictor

* Corresponding author. Tel. (O): +1-813-974-9036; fax: +1-813-974-5456.

E-mail address: toedores@csee.usf.edu (H.-N.L. Teodorescu).

[1] Romanian Academy.

0933-3657/00/$ – see front matter
PII: S0933-3657(00)00076-2

1. Introduction

1.1. Background

Tremor may be a disabling condition and affects a large number of people, mainly the elderly. The urgency of developing accurate diagnostic tools and means for treating tremor is related to the increase of the population affected by tremor. The US population above 65-year-old in 2005 is expected to be 24% — about five times the percentage 100 years ago [1]. The situation in US is still less developed than in several European countries, which, in turn, lag behind Japan. A comparison of the population segments in a representative selection of countries around the world is shown in Fig. 1, based on data found in [2]. The ''older old'' segment of the population, i.e. the segment aged above 80 years, becomes a significant part of the overall population in countries with life expectancy higher than 75 years (see Fig. 2, based on data in [2]). Rough estimations put the percentage of people in the *older old* segment affected by tremor between 25 and 40%. The need for extensive supply of advanced rehabilitation technology in general [3], and in the field of tremor specifically is acute and may become dramatic for industrialized nations, where the age expectation is believed to increase to 90 years in the next four decades. The elderly population's specific rehabilitation needs, including tremor related rehabilitation, have to be satisfied. Tremor treatment includes education of people with tremor to cope with their condition, medication, and prosthetic means to reduce tremor and to maintain and restore the functional abilities. In this paper, the tremor diagnosis and rehabilitation issues are being addressed.

1.2. Current state in tremor-related research

Tremor can affect the limbs, head, voice, and the whole body, as in posturographic tremor. It is widely recognized that, despite significant progresses in neurology, posturography, electromyography, and investigation techniques, ''tremor is commonly encountered in medical practice, but can be difficult to diagnose and manage'' [6]. Psychiatrists

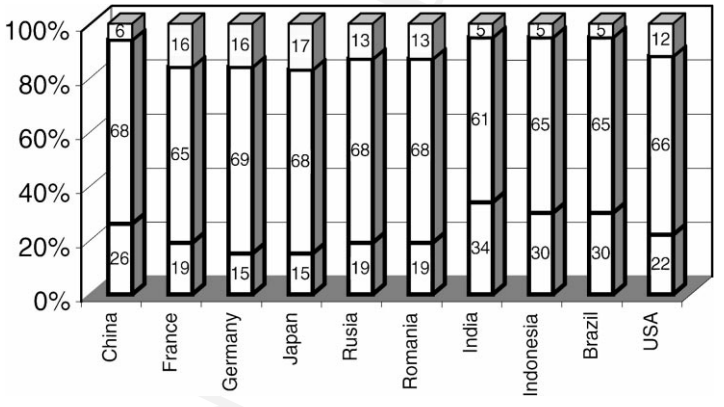

Fig. 1. Age segments in various countries.

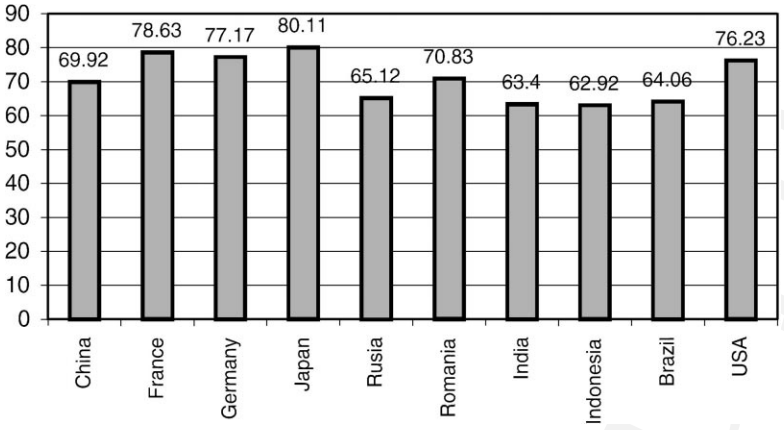

Fig. 2. Life expectancy at birth, in various countries.

are able to identify the types of tremor by visual inspection of the rest, postural and intention tremor, fatigue tests, and by other clinical signs, and recent research significantly advanced the field [7,8,10,14–21,25,26,28,31,34,42,43,45,48,61]. Differential diagnosis in tremor is still performed by clinical signs only, yet recently there is an increase in interest in tremor analysis using appropriate equipment. The essential tremor and the Parkinson tremor are the most common types of tremor. Rather frequent cases of misdiagnosis between different types of tremor are reported, for instance between intention tremor and cerebellar tremors [15], asking for improved tools to help diagnosis. Recently, several researchers have analyzed tremor as related to various diseases and proposed new analysis procedures [6–9,17,19,33,35,37,40,56]. Lauk et al. [33] have developed software for recording and analysis of human tremor. Lin and Zev Rymer [35] reported the analysis of pendular motion of the lower leg in spastic human subjects. Louis et al. [37,38] report on a portable instrument for assessing tremor severity in epidemiologic field studies. However, the techniques to measure and analyze tremor remain rather undeveloped and not widely accepted.

Beyond measuring tremor, the assessment of the functional disability it produces is needed for a correct evaluation of the subject rehabilitation needs and for choosing the appropriate rehabilitation methods. Several authors introduced methods to perform such an evaluation of the disability and of methods to assess it, e.g. [11,17,19,37,38,40]. In previously reported research [50,56], we have proposed the dynamic nonlinear analysis (chaos analysis) and new parameters to describe the tremor movements.

When the causes of tremor cannot be eliminated, natural or artificial tremor control is needed. Lundervold et al. [39] report on the reduction of tremor and related disability using behavioral relaxation training. Unfortunately, natural tremor control is poor because tremor is essentially an unconscious movement, moreover, as pointed out in [32], the natural thresholds for detection of limb movements is higher at frequencies corresponding to tremor, thus natural tremor detection is not taking place for low amplitude movements. The failure of noticing hand tremor asks for external feedback to be supplied for control

enhancement. Several researchers addressed the problem of providing artificial means to help subject apprehending the tremor for better control. Liu et al. [36], discussed the effects of visual feedback on manual tracking and action tremor in Parkinson's disease, while Lundervold et al. [39] discuss behavioral relaxation to reduce tremor. In [49,50], we addressed the problem of creating a visual and sound feedback related to tremor and the subject will be further developed in this paper. Because patient tremor control is not always effective, technical means to suppress the tremor are needed. One approach is to apply control to the central nervous system to control the tremor. This approach, addressing Parkinson treatment, has been analyzed by several researchers (e.g. [5]) and developed by Medtronic™ (see [4]). Another approach is to control the limb movements by applying electrical stimulations to the related muscles controlling the limb. This approach was independently introduced in [24,50] and is similar to the approach in [41].

Previously, we have proposed a new type of sensor to detect tremor and other movements [51,52]; also, we introduced several parameters to describe the tremor movements in limbs and related methods to analyze the tremor, and software tools to perform the analysis [50]. In addition, we analyzed chaos features in head tremor, mandibular tremor, and ''tremored voice'' and we presented applications related to rehabilitation and tremor control.

2. Measurement methods

2.1. Generalities

Tremor signal can be acquired using various techniques. Previously reported techniques used in tremor measurement are based on capacitive sensors, inductive sensors, 1-D or triaxial [18,19] accelerometric sensors and velocity sensors [40,44], resistive sensors [29], mechanical sensors [23], pressure-sensitive digitizing tablets [19] and optical sensors [23]. Image-based tremor measurement methods are also a strong candidate in the near future. Force and surface electromyogram (EMG) signals are frequently recorded and analyzed (e.g. [48]). The sensors used to measure the tremor should be carefully selected. For an elementary measurement, the sensor performance is not critical, as far as the sensor is low weight, or has non-contact measurement capabilities, to avoid loading the hand. However, when a nonlinear analysis is performed, low noise, high sensitivity, and high linearity sensors are required.

For the nonlinear analysis, the sampling frequency has to be much higher than the bandwidth of the noise, and the acquisition should be of high precision (at least 12 bits); else, the sampling and quantization noise generate unreliable results. The noise can destroy the very noise-sensitive nonlinear information in the signal and lead to incorrect results.

A specially designed sensor and measuring system have been used; these are based on a resonant sensor and on the commercial Tremor analyzer™ system, developed by T&T™ Ltd., according to our design [50,51,55,56]. The system measures the movement of the whole hand and can be adapted to measure the leg, jaw, and head tremor. Moreover, accelerometric sensors were used to measure individual finger tremor and the analysis can be complemented by electromyography, with additional equipment.

2.2. The sensor

A new type of sensor [51] which has the advantage of being unobtrusive and allowing us the measurement without contact to the subject hand has been used. The sensing element is a distributed RLC circuit that is tuned to, or close to, the predetermined frequency of a driving oscillator. The resonant sensor relies on an oscillator that couples through a relatively high-impedance to the sensing element a signal having a predetermined frequency. The high-impedance and the resonant sensor form a voltage divider circuit that generates at their junction a signal that is directly representative of a position and/or movement of an object in proximity to resonant sensor. The proximity of sensed object to resonant sensor causes a change in the parallel resonant frequency of resonant sensor, which causes corresponding changes in its impedance and, therefore, the magnitude of the signal across the resonant sensor.

In contrast to conventional inductor/capacitor (LC) circuits that intentionally minimize undesirable parasitic capacitances and couplings to surrounding objects, this type of sensor enhances the distributed capacitances and couplings and employs them as sensitive object-sensing elements. Suitable distributed capacitance and inductance for the resonant sensor are achieved by forming planar winding in a strip-like shape in which conductor width optimizes the electric and magnetic field distributions of the sensor. Planar winding has a relatively large conductor width and a relatively small spacing between successive turns to achieve a suitably high capacitance between the turns and a suitably large overall capacitance for resonant sensor. The ratio of spacing to conductor width should be kept low (1:1 or less) to maximize the distributed capacitance of resonant sensor. The winding is shaped to provide a relatively uniform electric field in an object-sensing zone that is generally determined by the overall dimensions and shape of resonant sensor. The dielectric substrate is planar and has a low relative dielectric constant, ranging from about 1.0 to about 5.0, to insure a high sensitivity of resonant sensor to proximal dielectric objects.

The resonant sensor behaves as a low-loss, high Q, distributed parallel RLC circuit having significant distributed capacitances, inductances, but low dissipation factors that contribute to enhanced electrical and magnetic coupling to the adjacent sensing zone. The sensor has a Q ranging from about 30 to about 100 under free conditions (no object in proximity). All of the distributed elements, R, L, C, are dependent on the proximity of surrounding objects and contribute to sensing the objects. Distributed capacitances and inductances (and possibly an external fixed capacitance) determine the resonant frequency of resonant sensor. Distributed losses in the equivalent capacitance and inductance, which are affected by dissipation in proximal objects, determine the Q and, therefore, the sensitivity of resonant sensor. Such an electrical field is suitable for sensing dielectric (nonconductive and nonmagnetic) objects, such as the hand.

Because of the proximity of object, the loaded impedance versus frequency function curve shifts and the resonant frequency of resonant sensor shifts away from the operating frequency, moreover the quality factor Q changes due to increased loses, thus producing a change of the sensor overall impedance. The shifting of the curve can be in either a higher- or lower-frequency direction depending on the sensor configuration. When a dielectric object is in proximity to resonant sensor, its equivalent capacitance increases, lowering its

resonant frequency relative to operating frequency. Consequently, the voltage divider output voltage level decreases. When a conductive object is proximal to resonant sensor, its equivalent capacitance and equivalent resistance increase, thereby lowering its Q and its resonant frequency relative to operating frequency. Consequently, the voltage divider voltage level decreases. As the human body contributes both a capacitance and an electric loss, both effects above described are present, and they contribute to the sensing process. The impedance change is measured to determine the distance to the object.

To minimize loading of the signal across resonant sensor, a high input impedance buffer amplifier, having a low input capacitance, conveys the signal to a detector that extracts a peak (or average) envelope voltage value from the signal. The voltage divider formed by high-impedance and resonant sensor provides an output voltage to buffer amplifier that is directly proportional to the impedance of resonant sensor at an operating frequency. The envelope voltage is conditioned by a band-pass filter and an amplifier to produce an analog output signal. The filter also removes power supply hum (50/60 Hz) and noise at frequencies >150 Hz. A linearization circuit is typically added to linearize the output voltage as a function of distance to object. A complete description of the sensor, including schematics and operation, are provided in [51].

2.3. Signal processing

Signal processing is done in two steps. First, the signal is pre-processed to remove the main perturbations. Then, the signal is processed in view of the analysis.

2.3.1. Pre-processing

The tremor is a complex movement, including components derived from respiration movements and other movements unrelated to tremor. The respiration contributes to the low frequency movements of the hand. These components should be removed, tacking into account that respiration has a basic frequency of about 0.1–0.3 Hz for adult subjects, with a bandwidth in the range 0.05–3 Hz. A high-pass filtering, at about 2 Hz, is recommended. Separate acquisition of the respiration signal may help removing this component by tuning an LP filter to the respiration signal or by using an adaptive signal canceling method. Similar means may be used to partly remove the movements induced by the blood flow. On the other hand, there is a random component in the movement, which bandwidth is difficult to determine in the present stage because of the chaotic component must also be considered. We estimate this bandwidth at frequencies higher than 10–40 Hz [56].

In our experiments, which are performed based on equipment built according to this description, the signal is low-pass pre-filtered and high-pass filtered at 40 and 0.1 Hz, respectively, with analogue filters. Then, the signal is sampled with a sampling frequency of 100 Hz and quantized to 12 bits, using a National Instruments™ acquisition board, which, together with the equipment for tremor sensing and a personal computer constitutes the hardware set-up in this application.

2.3.2. Signal characterization: linear analysis

Power spectra are computed using a 512 point fast Fourier transform, performed on each time window. Based on the Fourier spectrum in the 0–25 Hz range and on the amplitude–

time representation, several parameters are used to characterize the tremor signal. Derived parameters include the ''main frequency'', the periodicity index, the frequency spreading, the minimal and the maximal period, the peak and average amplitude, and the high-frequency content to low frequency content ratio, briefly named ''high-to-low ratio''. Some of these parameters are commonly used in tremor analysis, like amplitude and main frequency, some were adopted from other applications, like the ''low-to-high'' or LH index, and a few of the parameters were introduced specifically for this application.

We briefly explain the definition of these parameters. The ''main frequency'' is defined as the frequency corresponding to the highest peak in the Fourier spectrum. The ratio between the low frequency region and high frequency region energy in the spectrum is computed based on a boundary between the two frequency regions, set at 6 Hz. This frequency is generally assumed to lie about the middle between the ''low-frequency tremor'' and the ''high-frequency tremor'' [6,15].

The ''periodicity index'' is an ad hoc parameter, defined as the ratio between the power contents of the main peak in the spectrum and the total power in the signal. This index provides rough information on how much does the signal quasi-periodic component in tremor play a role. A low periodicity factor shows either that the signal includes more than one quasi-periodic component, thus having several causes, or that it is ''noisy''. The frequency spreading is computed as the spread of the components in the frequency spectrum. All these parameters are computed at the running time and displayed by the software that complements the equipment for diagnosis. A typical screen is shown in Fig. 3.

2.3.3. Signal characterization: nonlinear analysis

Previous research [56] indicates that tremor may include a significant nonlinear, chaotic component, which may play a part in diagnosis and rehabilitation. Here, the nonlinear analysis is performed to determine the correlation dimension and the Lyapunov (maximal) exponent, and a visual examination of the phase diagram is available at running time in the software (Fig. 3). A positive Lyapunov exponent is known to be the primary indicator of a chaotic dynamics. It relieves the degree of divergence of the ''trajectories'', that is, the initial condition sensitivity and unpredictability of the signal. The low values of the Lyapunov exponent show a ''weakly-chaotic'' regime (weakly divergent trajectories). The maximal Lyapunov exponent (and the correlation dimension, reported subsequently) is computed for time series of 2400 samples from the recordings. The values of the Lyapunov exponent range from almost 0 (0.05) to 0.7. The results do not show significant differences in the Lyapunov exponents for young and healthy subjects, when contrasted to the group of about 45-year-old people we have tested.

Another parameter frequently used to characterize chaotic behaviors is the correlation dimension. We determined that the correlation dimension D of the tremor signal is in the range [0.5; 5]. Most recordings exhibit a D value in the range [2.5; 3]. The range of D is somewhat higher for the signal acquired under conditions without muscular effort than under muscular effort. High differences in the correlation dimension of the signal have been found for several young subjects, possibly showing that this parameter — and the tremor complexity — is not specific to a subject, but rather to his or her state.

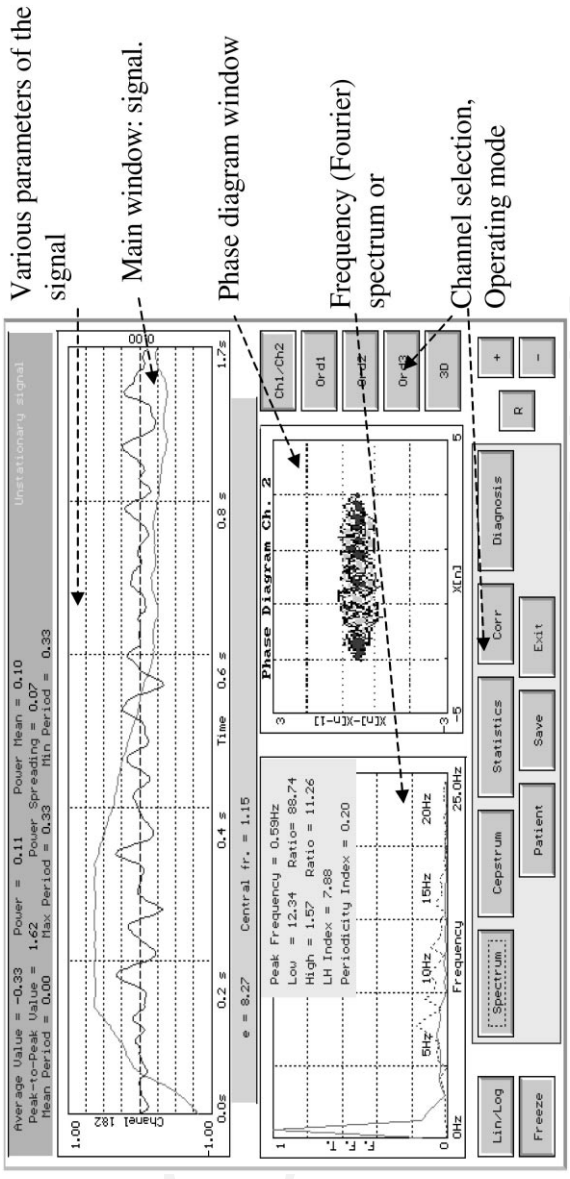

Fig. 3. Main screen snapshot of the basic program for signal acquisition and processing (reproduced with permission, *Techniques & Technologies, Ltd.*).

2.4. Data acquisition conditions

Subjects were asked to keep fixed the arm making an angle of about 20° with the horizontal (under the horizontal); this position is considered somewhat more natural and less tiring than the horizontal position, usually assumed in other tests. The subject is seating during measurements. For the duration of the experiments (1–3 min), subjects had to maintain the same position of the hand. Fatigue is expected to influence the last part of the determinations. Therefore, the analysis for ''normal condition'' is performed only for the first minute, while the analysis for ''fatigue condition'' is performed on the last minute. In another set of experiments, the subjects were required to hold in their hand an object (weigheing about 1 kg), such that muscular effort and fatigue is forced upon, for analyzing the fatigue effect on tremor [16,56]. Normal subjects with ages ranging from 20 to 45 years were tested, as well as alcoholic subjects (for details on the method, see [51,56]).

3. Tremor characterization for fuzzy knowledge bases in diagnosis and rehabilitation

Automatic diagnosis and the use in rehabilitation systems are two major applications of tremor analysis. The realization of feedback in tremor-related rehabilitation is a major objective of the tremor analysis. The feedback has to be simple enough for easy understanding and learning. It should make use of easy to grasp visual and audible information. In this purpose, the information has to be appropriately compressed.

Several groups have recently investigated graphical interfaces in systems aimed to rehabilitation. Toth-Cohen et al. [57] analyzed various computer-assisted instruction programs in hand therapy. Although their study focuses on the therapists, not the patients, it reveals some useful hints to improve the interaction with the patient as well.

For rehabilitation purposes, the use of a fuzzy knowledge base has been proposed [49,50,56]. The knowledge base includes rules referring to both the classic and chaotic features of the signals, because the classic parameters alone may not consistently represent the whole tremor process. Fuzzy logic received a significant attention in medical sciences and a large number of medical applications were solved using fuzzy systems, from control to diagnosis to medical image processing [55–57].

The main parameters and the corresponding linguistic degrees used in the rule base are presented in Table 1. The number of linguistic degrees is primarily dictated by medical knowledge, i.e. by the meaning that can be assigned to the different linguistic degrees and to the corresponding tremor classes, as identified by the resulted set of parameters. For example, at present, it appears to be meaningless to use more than two degrees for the Lyapunov exponent, as no medical meaning can be derived, except that an almost non-chaotic tremor is less complex than a movement with high Lyapunov exponent value. The degrees of understanding of the meaning of these parameters by the physicians and of grasping the meaning by the average subject are varying (see Table 1). The best understood and comprehended are the amplitude and the (main) frequency. Physicians mostly insist on the frequency parameter, as it is known to vary with and to provide strong indications on the type of tremor, thus helping diagnosis.

Table 1
The main parameters and the corresponding linguistic degrees

Parameter	Notation	Number of linguistic degrees	Notation for the linguistic degrees	Remarks
Amplitude	*A*	3	Low, average, high	Well understood by physicians and comprehended by subjects
Main frequency	*F*	4	Low, average, high, very high	Well understood by physicians and comprehended by subjects
''Low-to-high'' ratio	LH	3	Low, average, high	Well understood by physicians but poorly comprehended by subjects
Periodicity index	PI	3	Low, average, high	Well understood by physicians but poorly comprehended by subjects
Frequency spreading	FS	3	Low, average, high	Partly understood by physicians but poorly comprehended by subjects
Correlation dimension	*D*	3	Low, average, high	Partly understood by physicians but poorly comprehended by subjects
Lyapunov exponent	*L*	2	Small, large	Poorly understood by physicians and poorly comprehended by subjects

With the purpose of creating an easy to grasp feedback that helps patients to become aware of the characteristics of the tremor of their limbs, moreover to help them controlling the tremor, we have proposed [51,56] a representation of the tremor by images and sounds. This representation is synthetic and is based on the linguistic and fuzzy valuation of the main parameters of the tremor. The use of linguistic and fuzzy valuations is justified by its simplicity (easy to understand by the physician and the patient), moreover by good information compression.

In one of the available versions of the system, the feedback is realized by showing on the computer screen a simplified version of the screen in the full-research program, as in Fig. 3. In other versions, for feedback purpose, the display shows a ball moving over a plane at the speed of the hand tremor, as well as one or two analog meters. An analog meter (see Fig. 4) shows either an average of the squared tremor amplitude, or an evaluation of the tremor amplitude performed according to a set of rules explained subsequently. In case of the screen showing two analog meters, the left-side analog meter shows the value of the fused amplitude, while the right-side bar meter can be used to display actual vertical movement, or the evolution of the fused irregularity index, or the evolution of another parameter.

The fusing of the numerical parameters derived from the analysis is performed based on fuzzy aggregation. The evaluation of the amplitude is dependent on the ''aggravating factors'', for instance frequency of tremor, and tremor irregularity measures.

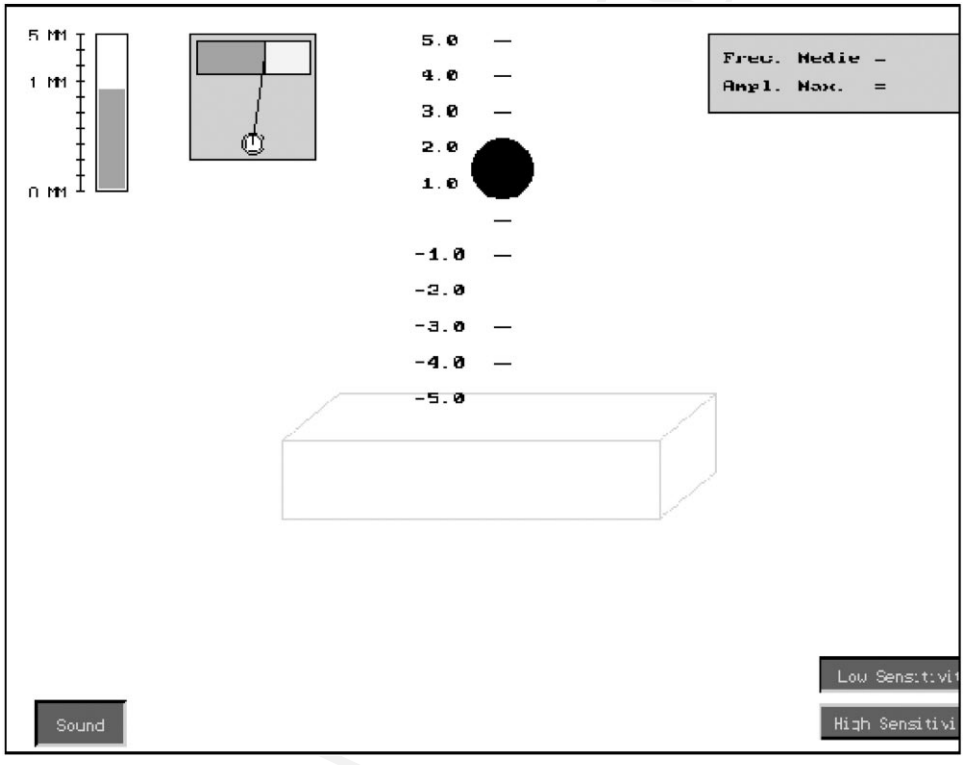

Fig. 4. Example of display available for the feedback.

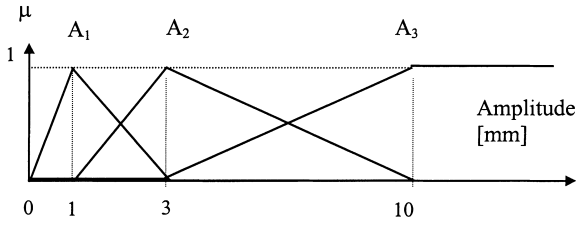

Fig. 5. Membership functions for tremor amplitude A_1 = low; A_2 = average; A_3 = impairing.

To reduce the number of represented parameters, yet preserving the essential information, we performed the fusing into two parameters of the numerical parameters derived from the analysis. The primary parameter ''amplitude'' is not eliminated, because its meaning is easy to grasp; however, it is modified to include information related to other parameters, regarded as ''aggravating factors''. Indeed, the medical understanding is that a certain amplitude value may be more or less incapacitating, depending on other features of the tremor. Therefore, such features are viewed as aggravating factors and are fused in an ''equivalent amplitude'' factor, used in the feedback under the name ''amplitude''. Namely, the evaluation of the amplitude is modified by the frequency of the tremor, and by several parameters related to tremor irregularity. The contribution of theses factors is determined, at this level, purely empirically, based on medical experts' opinions. Examples of the membership functions used for two parameters are shown in Figs. 5 and 6. Similarly, a global parameter related to tremor ''irregularity'' is defined.

The rules in the rule base used to globally characterize the tremor are in the generic form:

If	amplitude A is in the range (A_1–A_3)
and	main frequency F is in the range (F_1–F_4)
and	HL index is in the range (HL_1–HL_3)
and	periodicity index PI is in the range (P_1–P_3)
and	correlation dimension D is in the range (D_1–D_3)
and	Lyapunov exponent L is (low, high)
then	amplitude–frequency (fused) parameter AF is (AF_1–AF_5)
moreover	irregularity (fused) parameter IRREG is (IRR_1–IRR_3).

The parameters AF and IRREG are fuzzy (fused) features of the movements. As an example, the first rule in the system is

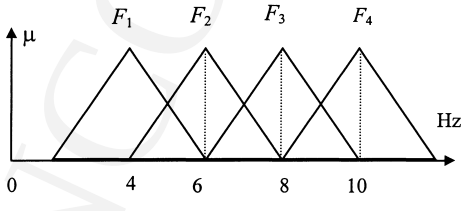

Fig. 6. Membership functions for the ''main frequency'' of the tremor.

If A is A_1 = low *and F* is F_1 = very low *and* HL is HL_1 = *l*ow *and* PI is P_1 *and D* is D_1 *and L* is low
then AF is AF_1 (very low).

However, the computation of the output membership functions is performed based on an empirical correction to the MIN aggregation of the premises, using coefficients to trim the result. For instance, the membership function of AF is

$$\mu_{AF}(a,f,u,v,d) = \min[\lambda_1\mu_A(a),\ \lambda_2\mu_F(f),\ \lambda_3\mu_{HL}(u),\ \lambda_4\mu_{PI}(v),\ \lambda_5\mu_D(d)]$$

Here, $\lambda_1, \lambda_2, \lambda_3, \lambda_4, \lambda_5 \in [0,1]$ are coefficients appropriately chosen (empirical choice). The need for the λ coefficients is dictated by the fact that at present stage it appears that medical experts may partly agree on the membership functions of the premises and on the rules, but the result obtained by *min* operations should be adjusted to receive the agreement of the experts. Therefore, a corrected version of aggregation was found appropriate. The λ coefficients are chosen strictly empirically.

The rules establish the relationships between premises and consequences (the appropriate linguistic degrees, derived by empirical methods.) The resulted parameters AF and IRREG are synthetic fuzzy features of the movements. The results of the inference described above are defuzzified and used in the feedback to build the image of the analog indicator on the display.

There are various feedback facilities under current evaluation with the system. In one of them, the feedback is realized by showing on the computer screen a simplified version of the screen used in the full-research program. In another version, a screen showing a ball that synchronously follows the vertical tremor of the hand. Optionally, the ball has the diameter and color representing two other parameters. Moreover, an analog indicator is used for the feedback purpose. The analog indicator shows either an average of the tremor amplitude, or an evaluation of the tremor amplitude performed according to the rule base. A sound is also generated every time the tremor fused amplitude is higher than a specified threshold.

Yet, another representation currently being considered makes use of a four-dimensional space, namely: color of the background, color of the spot, dimension of the spot, and position of the spot on the background screen. This representation uses four fused parameters, not described in detail here. The color of the spot represents a third fused parameter, named ''fused frequency'' (FDF), that includes information on the main frequency and on the irregularity of the movement. The color of the screen shows the IRREG parameter; for example yellow for very irregular, light gray for average and dark gray for very regular. The dimension of the spot represents a forth variable, showing progress in control and is activated only for subjects having a ''history'' in the database. A squeezing spot shows improvement of control; an inflating spot shows decrease of performance; the position of the spot on the screen shows the relative amplitude and frequency of the tremor signal. The patient, in cooperation with the therapist, can modify some of the features, such as the sensitivity and the limit frequency in the LH index, or the dimension of the spot for a given value of the amplitude.

We also have analyzed other representations for the feedback, including a representation based on temporal (dynamical) fuzzy sets analysis. The principles of temporal fuzzy sets and of the related representation are given in [30,47]. Using a fuzzy information space

representation has been found useful for diagnosis purposes. Namely, we have presented a way to characterize the attractors corresponding to the hand tremor using the method of classification based on temporal fuzzy sets. However, the method is yet of rather limited use in feedback, because of the high complexity of the generated figures. Further research will be conducted to improve the use of this method in graphical interfaces, possibly by simplifying the representation.

4. Tremor prediction

In order to increase the rehabilitation capabilities of the subject based on feedback, it is preferable to provide a feedback that includes information on the just-to-come movement, not on the present-moment movement. This requires a prediction of the movement. Moreover, when the rehabilitation based on subject's control is not effective, a different control strategy must be adopted, for example using an external control loop and electrical stimulation of the muscles. This approach is presented in the present section. We have developed several predictors, including multi-layer perceptron neural predictors [9,55], feature-oriented neural predictors [55] and neuro-fuzzy predictors [12]. Here, we present the neuro-fuzzy predictor and briefly compare the results with other predictors.

4.1. A neuron with fuzzy synapses

The use of fuzzy and neuro-fuzzy prediction of time series has recently became popular [27,53,54,59]. In this section, we investigate the use of a specific type of neuron, named neuron with fuzzy synapses (NFS), to the prediction of tremor movements. For a NFS having m inputs, x_1–x_m, the output y is computed as a sum of nonlinear functions:

$$y = \sum_{i=1}^{m} f_i(x_i), \quad f_i : U_i \to R,\ U_i \subset R \tag{1}$$

A function f_i can be viewed as a synaptic transformation of its input x_i. Since every function f_i is implemented using a particular class of neuro-fuzzy systems, we shall use the term fuzzy synapse (FS) to designate these particular synapses. The fuzzy synapse number i, implementing the NFS function f_i from Eq. (1), uses a number of N reference fuzzy sets, denoted with A_{ir}, $r = 1, 2, \ldots, N$. Every fuzzy set A_{ir} is characterized by its membership function (MF) $\mu_{A_{ir}} : U_i \to [0, 1]$.

The membership functions $\mu_{A_{ir}}$ have a triangular form, like in Fig. 7, where four MFs are depicted. For a certain value u_i of the input x_i, the truth degree (TD) t_{ir} of the proposition (x_i is A_{ir}), is equal with the value of MF $\mu_{A_{ir}}$ computed for u_i, $t_{ir} = \mu_{A_{ir}}(u_i)$. For every crisp input value, a number of N truth degrees t_{ir}, $r = 1, 2, \ldots, N$, are computed. But, as one can see from Fig. 1, only two consecutive TDs are nonzero. Moreover, the sum of these TDs is 1, $t_{i,k} + t_{i,k+1} = 1$, where k is the index of the first nonzero TD.

The fuzzy synapse has N rules, $r = 1, 2, \ldots, N$, of the form:

$$\text{If } x_i \text{ is } A_{ir} \text{ then } y_{ir} = w_{i1r} t_{ir} + w_{i2r} t_{ir}^2 + \cdots + w_{iPr} t_{ir}^P \tag{2}$$

where y_{ir} is the output of the rule r, $w_{ijr}, j = 1, 2, \ldots, P$, are adaptive weights of the rule r, t_{ir} is the truth degree of the rule premise (x_i is A_{ir}), $t_{ir} = \mu_{A_{ir}}(x_i)$.

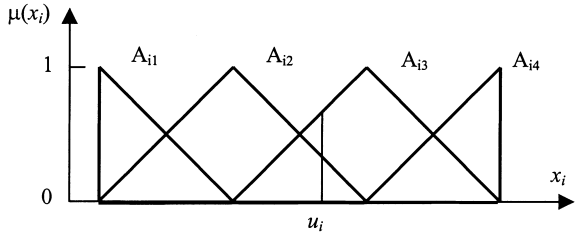

Fig. 7. Triangular membership functions of the fuzzy reference sets. For every input value, u_i, only two truth degrees are nonzero.

The function used for the rule output computation is a polynomial of degree P, having the variable t_{ir} and the coefficients w_{ijr}. For $P = 1$, Eq. (2) defines the fuzzy rule of Yamakawa's neuron synapse [60]. Despite its computational simplicity, Yamakawa's neuron provides good prediction performances for the tested series. For polynomials of degree $P > 1$, there is an increase in the computational complexity of the rule compared to the case $P = 1$, but the improved prediction performances justify the increase in computational complexity [12].

We present the prediction performances of predictor schemes based on neurons with fuzzy synapses of order $P = 3$ in tremor prediction applications. The rules of these particular synapses are, for the third-order fuzzy synapse:

$$\text{Rule no. } r: \quad \text{If } x_i \text{ is } A_{ir} \text{ then } y_{ir} = w_{i1,r}t_{ir} + w_{i2,r}t_{ir}^2 + w_{i3,r}t_{ir}^3$$

The output of the fuzzy synapse, $y_i = f_i(x_i)$, is computed as the linear combination of the rule outputs y_{ir}

$$y_i = f_i(x_i) = \frac{\sum_{r=1}^{N} y_{ir}}{\sum_{r=1}^{N} t_{ir}} = \frac{\sum_{r=1}^{N} y_{ir}}{\sum_{r=1}^{N} \mu_{A_{ir}}(x_i)} \tag{3}$$

where y_{ir} is computed with Eq. (2), and N the number of the synapse rules. The fuzzy synapse is a fuzzy system with a crisp input x_i and a crisp output y_i, belonging to the category of Sugeno fuzzy systems. The parameters of the fuzzy synapse are the weights w_{ijr} from Eq. (2). By adapting these weights, we can approximate a desired shape of the synapse function f_i.

For every value belonging to the input domain U_i, only two adjacent rules have nonzero truth degree, and the sum of the truth degrees is equal to one. By denoting with $t_{ik} = \mu_{Aik}(x_i)$ and $t_{i,k+1} = \mu_{Ai,k+1}(x_i)$, these nonzero truth degrees, we can rewrite Eq. (3) as $y_i = y_{ik} + y_{i,k+1}$. Thus, for triangular MFs, the computation is drastically reduced. Since the computation complexity does not depend on the number of fuzzy rules N, one can use as many fuzzy reference sets as needed, for a satisfactory fuzzy partitioning of the input domain U_i.

We denote $a_1 = x_{\min}, a_2, \ldots, a_r, \ldots, a_N = x_{\max}, a_1 < a_2 < \cdots < a_r < a_N$, the points in the input domain U_i where the triangular MFs are unitary, $\mu_{A_{ir}}(a_r) = 1, r = 1, 2, \ldots, N$. For Yamakawa's neuron, one can show that between any two successive points a_r, the synapse output y_i, computed with Eq. (3), has a linear variation with x_i, that is

$y_i = c_{0r} + c_{1r}x_i$, for $x_i \in [a_r, a_{r+1}]$, $r = 1, 2, \ldots, N-1$. For a third-order synapse, the synapse output y_i has a third-order polynomial variation with the input x_i, on the intervals $[a_r, a_{r+1}]$. The nonlinear behavior of the higher (second and third)-order synapses allows us better prediction performances with respect to Yamakawa's neuron performances [12], with the expense of increased computational complexity.

The neuron output is the sum of all fuzzy synapses outputs. Thus, one can write the neuron output y, for a particular input vector $(u_1, u_2, \ldots, u_m)$, as

$$y = \sum_{i=1}^{m} f_i(u_i) = \sum_{i=1}^{m}\sum_{r=1}^{N} y_{ir}(u_i) = \sum_{i=1}^{m}\sum_{r=1}^{N}\sum_{j=1}^{P} w_{ijr}[t_{ir}(u_i)]^j \tag{4}$$

Since the TDs t_{ir} are directly computed for a certain input value, Eq. (4) represents a linear weighted sum of dimension $m \times N \times P$, having the weights w_{ijr}. Adapting these weights can approximate the desired behavior of the neuron synapses.

4.2. The training algorithm of the neuron with fuzzy synapses

From Eq. (4), it results that the NFS is a linear neuron (an ADALINE neuron), having the weights w_{ijr} and the "inputs" $(t_{ir})^j$. For the weights computation of the linear neurons, it is convenient to apply the least mean square (LMS) algorithm. The LMS algorithm computes the neuron weights such that the energy of the instantaneous error between the desired neuron output $d(k)$ and the current neuron output $y(k)$ is minimized. If we denote the instantaneous error by e(k), $e(k) = d(k) - y(k)$, the instantaneous energy error is $E(k) = e^2(k)$. The neuron weights are computed such that the partial derivatives of $E(k)$, with respect to the weights, are 0

$$\frac{\partial E(k)}{\partial w_i} = 0, \quad i = 1, 2, \ldots, N_i \tag{5}$$

where w_i are the weights, and N_i the number of weights. Applying Eq. (5) for NFS, the neuron weight w_{ijr} is computed as

$$w_{ijr}(k+1) = w_{ijr}(k) + \eta(k)[d(k) - y(k)]\{t_{ir}[u_i(k)]\}^j \tag{6}$$

where $d(k)$ is the desired output of the neuron, $y(k)$ is the neuron output computed with Eq. (4), k is the iteration number, and $\eta(k)$ regulates the LMS algorithm convergence speed. For every input $u_i(k)$, only two LMS equations are used per synapse, because the truth degrees t_{ir} are nonzero only for two consecutive rules.

The LMS algorithm is convergent when $\eta(k)E < 1$, where E is the mean energy of the neuron inputs. A practical implementation of this condition is given by the equation

$$\eta(k) = \frac{\beta}{E_{\text{in}}(k)} \tag{7}$$

where $0 < \beta < 1$, and $E_{\text{in}}(k)$ is an estimate of the inputs energy. The neuron inputs are (t_{ir}), and their energy estimate $E_{\text{in}}(k)$ is computed recursively as

$$E_{\text{in}}(k) = (1-\alpha)E_{\text{in}}(k-1) + \alpha\sum_{i=1}^{m}\sum_{r=1}^{N}\sum_{j=1}^{P}\{t_{ir}[u_i(k)]\}^{2j} \tag{8}$$

where $0 < \alpha < 1$. We have used the values $\alpha = \beta = 0.5$.

4.3. Chaotic series prediction with NFS

The m past samples, $x(n-p)$, $x(n-p-1), \ldots, x(n-p-m+1)$, of the tremor time series $x(n)$, are the neuron inputs, in the case of a p-steps prediction. The output $y(n)$ of the neuron is an estimate of the current time sample $x(n)$

$$x(n) \approx y(n) = \sum_{i=1}^{m} f_i[x(n+1-p-i)] \tag{9}$$

where $x(n)$ is the time series, p the prediction step and f_i, $i = 1, 2, \ldots, m$, are the neuron's synaptic functions.

In Fig. 8, a schematics of a five-step predictor, $p = 5$, is presented. Every delay cell, denoted by D, delays its input with one time sample. Five delay cells are used to obtain the first NFS input, $x_1(n) = x(n-5)$, and then single delay cells are inserted between the NFS inputs to obtain the neuron inputs x_2–x_m. The past samples $x(n-5)$, $x(n-6), \ldots,$ $x(n-m-4)$ are the inputs of the neuron. The neuron fuzzy synapses FS_1, FS_2, to FS_m are trained such that its output $y(n)$ approximates the series $x(n)$. D represents unitary delay cells. This prediction scheme is common to other neural networks based prediction methods for chaotic series, where NFS is replaced by other adaptive structures, able to play the role of a universal approximator, like multi-layer perceptrons, 'radial basis functions' networks or some neuro-fuzzy systems [13,22,58,59].

The time series samples arrive to the neuron inputs at different moments of time, because of the time delay cells D. Since the neuron inputs are the samples of the same time series,

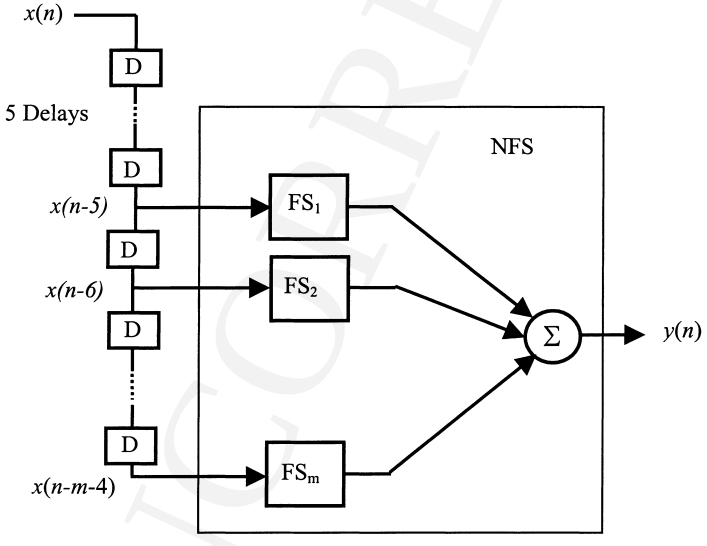

Fig. 8. A five-step predictor based on a neuron with fuzzy synapses.

one can use the same universe of discourse U for all the fuzzy synapses, FS_1 to FS_m. Thus, the universe of discourse U is the interval $[x_{\min}, x_{\max}]$, where $x_{\min}$ is the minimum series value, and $x_{\max}$ the maximum series value, computed over the time interval where prediction is made. It is reasonable to use identical MFs for all the inputs, that is, for all inputs x_i, $A_{ir} = A_r$.

A sliding window of consecutive samples of the chaotic series is used for the neuron training. To compute the weights w_{ijr} with the LMS algorithm Eqs. (6)–(8), we use M known successive samples $x(0)$, $x(1), \ldots, x(M-p)$, where $M \gg m$, M is the sliding window length, and m is the number of neuron inputs. After the weight computation, the trained neuron approximates the sample $x(M)$ as

$$x(M) \approx y(M) = \sum_{i=1}^{m} f_i[x(M+1-p-i)] \tag{10}$$

where p is the predictor step, and m the number of neuron inputs. For the prediction of the next sample $x(M+1)$, one computes the coefficients w_{ijr} using the samples $x(1), x(2), \ldots, x(M+1-p)$, and so on. The value of M is dictated by the nature of the chaotic series. Best results are obtained when M is bigger than the period of the lowest periodic component of the series.

4.4. Predictor performance estimation

To estimate the prediction performance, we use the statistics of the prediction error, and the normalized root mean square (RMSN) of the prediction error, defined as

$$\mathrm{RMSN} = \frac{\sqrt{\sum_{n=1}^{N_s}[d(n) - y(n)]^2}}{\sqrt{\sum_{n=1}^{N_s} d(n)^2}} \tag{11}$$

where $d(n)$ is the sequence to be predicted, $y(n)$ the predictor output, and N_s the number of predicted samples. The histogram of the prediction error is an intuitive indication of the quality of the prediction process. For a good prediction, the error should be close to white noise (Gauss probability distribution.) The normalized dispersion (DN) of the prediction error, that is the dispersion of the prediction error divided to the value range of the time series, is used together with the RMSN to illustrate numerically the prediction performances.

4.5. Prediction results

For the control purpose, as well as for training in rehabilitation, the prediction should be at least three steps in advance, to allow for the control is applied and to compensate at least partly for the inertia of the arm/hand. A five-step-ahead prediction is a reasonable trade-off between prediction error and feedback application lag. With a low sampling frequency to account for the slower movements represented by the main frequencies in the tremor spectrum (under 15 Hz), assuming a 50 Hz sampling in the control application, five-step-ahead prediction insures about 100 ms to apply control.

For the results presented in this paper, all neurons have three inputs and are third-order neurons with three MFs for each input. Results obtained for a five-step prediction are briefly presented here. In all prediction tests, the number of recorded samples is 992 and the training window includes 32 samples. The results include estimation of the prediction quality by the RMSN error, mean error, error dispersion, and the DN coefficient (error dispersion/series range). The results are contrasted with our previous results, obtained by applying MLP neural networks and feature-oriented neural predictors, as described in [9,55]. The fuzzy neuron is found to have advantages as simplicity and in many cases generates significantly lower prediction errors.

Fig. 9 illustrates an example of prediction. The trace of the actual tremor signal and the predicted signal are almost superposing. The prediction error signal is also shown on the same graph. The correlation function for the actual signal and for the signal predicted using the neuro-fuzzy predictor are depicted in Fig. 9. For various predictions, the mean error was between 0.0001 and 0.003, while the RMS error in the range 0.1–0.2. The histogram of the error shown in Fig. 10 demonstrates that the condition of Gaussian distribution of the error is satisfied. The autocorrelation functions of the actual and predicted signals, shown in Fig. 11, are almost identical, demonstrating that the essential information in the original signal is correctly imbedded in the predicted signal.

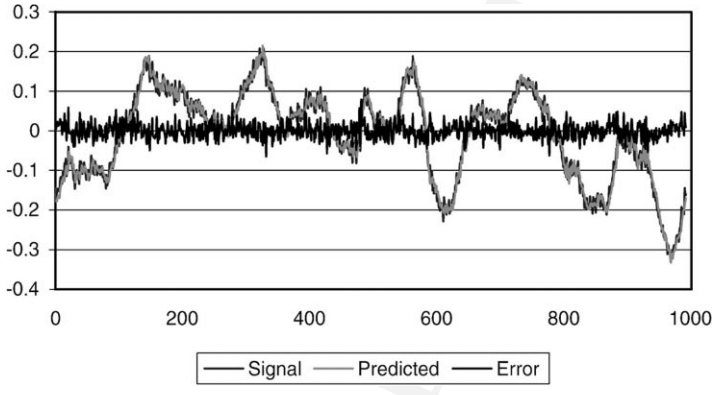

Fig. 9. Original signal, predicted signal, and error signal for a normal subject (Series A).

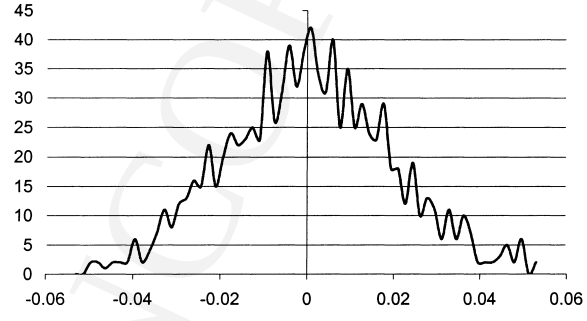

Fig. 10. Histogram of the error, for the signal in Fig. 9 (Series A).

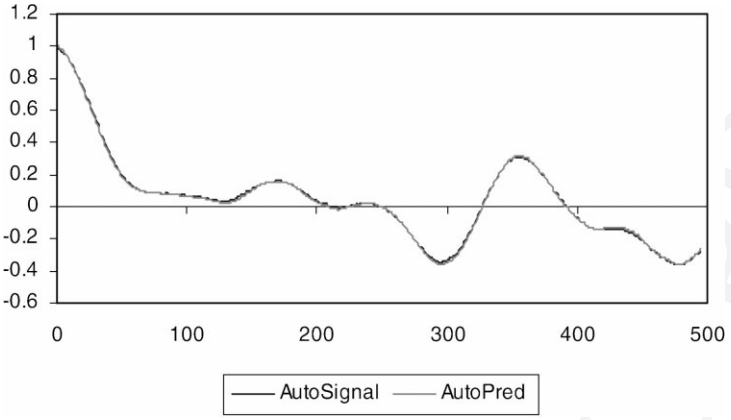

Fig. 11. Auto-correlation function of the original and predicted signal, respectively, for the signal in Fig. 9 (Series A).

Examples of numerical results corresponding to the figures in this section are shown in Table 2. Interesting enough, there is no visible correlation between the determined Lyapunov coefficients, or correlation dimension in the series and the prediction mean error or prediction error dispersion. This means that the fuzzy neuron predictor is very robust with respect to changes in the complexity of the chaotic process. This preliminary conclusion, however, should be supported by a larger data set evaluation. There was no visible decrease in performance when the predictor was used for data collected from an alcoholic subject, with comparison to normal subjects. (Alcoholic subjects show a different frequency spectrum and a specific tremor.)

Compared to a MLP predictor of similar complexity, as reported in [9,55], this predictor has better performances. Compared to the feature-space predictor presented in [55], the performances are almost the same, but the complexity of the neuro-fuzzy predictor is much lower, moreover the learning period significantly shorter for the same error (32 samples, compared to more than 100 samples).

Implementing the predictor in the feedback for rehabilitation will be attempted in the near future. On the other hand, for muscular control, finding a robust, accurate and simple predictor for the tremor signal solves only the initial part of the problem. Based on the predictor, an efficient muscular control has to be determined, implemented, and tested on subjects with various types of tremor.

Table 2
Numerical results of the series

Results	Series A	Series B	Series C	Series D
Range (amplitude)	−0.32 to 0.21	−0.14 to 0.21	−0.38 to 0.32	−0.32 to 0.39
RMS error	0.175808	0.111148	0.111052	0.1436
Error mean	0.00052	0.000196	−0.00221	−0.0024
Error dispersion	0.019382	0.009522	0.017088	0.019795
Error dispersion/series range	0.006	0.045156	0.045481	0.050821

5. Discussion and conclusions

In this work, we have presented an extensive research, including applications of fuzzy systems in the field of tremor rehabilitation, primary aimed to products. The first application is based on linear and nonlinear (chaos) analysis and the use of fuzzy logic in the assessment of tremor and related functional disabling, while the second application is related to tremor prediction in view of rehabilitation, and control. We have described a complete methodology for tremor analysis, including classic and chaotic parameters. A combination of linear and nonlinear analysis, supplemented by a data fusing using fuzzy methods is a good choice to create feedback in rehabilitation.

Although fuzzy logic is not the only way to solve the problems in hand, it clearly demonstrates certain advantages. The use of fuzzy logic considerably simplified the task of fusing the tremor parameters into a few parameters that can be represented in feedback. Moreover, the use of fuzzy logic bridges the gap between medical knowledge, patient comprehension of the feedback information and engineering signal processing methods.

One of our goals is the developing of predictive feedback and electric muscular control for tremor cancellation, for the cases when tremor control by the subject cannot be improved. The first step in developing such control is to insure a good predictor. We have compared several neural and neuro-fuzzy predictors, to insure a good trade-off between prediction capabilities, speed and complexity. Several results using MLP and feature-based neural predictors have been reported elsewhere [9,55], while in this paper we report on a predictor based on a generalized Yamakawa's neuron. As for the trade-off between precision and complexity, this predictor shows advantages over the two previously reported tremor predictors.

The experience gained in this extensive research taught us that the benefits of using fuzzy systems may be case-dependent and a mixture of design and implementation simplicity and improved performance may, sometime, justify the use of fuzzy systems. The improvement of the efficacy of computer-based tremor analysis, including nonlinear analysis, and improvements in the feedback provided to patients for rehabilitation purposes are seen as the major results in the present research.

Uncited reference

[46].

Acknowledgements

Most of the research performed by the first author was supported by *Techniques & Technologies* (*T&T*) Ltd. *T&T* Ltd. has provided several measuring set-ups and software, and largely covered the research expenses. The contribution of the third author was supported by the USF Center for Software Testing, under USF 2108-004.

References

[1] Population Profile of the United State 1995. Current Population Reports — Special Studies Series 23–289, US Department of Commerce — Bureau of the Census, July 1995, www.census.gov/population/pop-profile/p23-189.pdf.

[2] Country listing www.odci.gov/cia/publications/factbook/country.html.

[3] AATE document Empowering older and disabled people in the EU, 3 March 1997, www.fernuni-hagen.de/FTB/aaate/position.html.

[4] www.medtronic.com/intl/kinetra2.html, also www.medtronic.com/neuro/ncond/tremor.html.

[5] Alesch F, Pinter MM, Helscher RJ, Fertl L, Benabid AL, Koos WT. Stimulation of the ventral intermediate thalamic nucleus in tremor dominated Parkinson's disease and essential tremor. Acta Neurochir (Wien) 1995;136(1/2):75–81.

[6] Anouti A, Koller WC. Tremor disorders. Diagnosis and management. West J Med 1995;162(6):510–3.

[7] Arihara M, Sakamoto K. Evaluation of spectral characteristics of physiological tremor of finger based on mechanical model. Electromyogr Clin Neurophysiol 1999;39(5):289–304.

[8] Bain PG, Findley LJ, Britton TC, Rothwell JC, Gresty MA, Thompson PD, Marsden CD. Primary writing tremor. Brain 1995;118(6):1461–72.

[9] Bonciu C, Teodorescu HN. Prediction of a weakly chaotic signal using a MLP network in the features space. Int J Chaos Theory Appl 1998;3(3):35–9.

[10] Britton TC. Essential tremor and its variants. Curr Opin Neurol 1995;8(4):314–9.

[11] Cenk Akbostanci M, Ulkatan S, Yigit A, Aydin N, Mutluer N. Difference of disability between electrophysiologic subgroups of essential tremor. Can J Neurol Sci 2000;27(1):60–4.

[12] Chelaru IM. Chaotic series forecasting by neurons with fuzzy synapses. Int J Chaos Theory Appl 1999;4(4):47–57.

[13] Cybenko G. Approximation by superposition of sigmoidal function. Math Control Signals Syst 1989;2:303–14.

[14] Deuschl G, Heinen F, Guschlbauer B, Schneider S, Glocker FX, Lucking CH. Hand tremor in patients with spasmodic torticollis. Mov Disord 1997;12(4):547–52.

[15] Deuschl G. Differential diagnosis of tremor. J Neural Transm Suppl 1999;56:211–20.

[16] Ebenbichler GR, Kollmitzer J, Erim Z, Loscher: WN, Kerschan K, Posch M, Nowotny T, Kranzl A, Bochdansky T, Wober C. Load-dependence of fatigue related changes in tremor around 10 Hz. Clin Neurophysiol 2000;111(1):106–11.

[17] Edwards R, Beuter A. Indexes for identification of abnormal tremor using computer tremor evaluation systems. IEEE Trans Biomed Eng 1999;46(7):895–8.

[18] Elble RJ, Higgins C, Leffler K, Hughes L. Factors influencing the amplitude and frequency of essential tremor. Mov Disord 1994;9(6):589–96.

[19] Elble RJ, Brilliant M, Leffler K, Higgins C. Quantification of essential tremor in writing and drawing. Mov Disord 1996;11(1):70–8.

[20] Erimaki S, Christakos CN. Occurrence of widespread motor-unit firing correlations in muscle contractions: their role in the generation of tremor and time-varying voluntary force. J Neurophysiol 1999;82(5):2839–46.

[21] Ferraz HB, De Andrade LA, Silva SM, Borges V, Rocha MS. Postural tremor and dystonia. Clinical aspects and physiopathological considerations. Arq Neuropsiquiatr 1994;52(4):466–70.

[22] Girossi F, Poggio T. Networks and the best approximation property. Biological Cybernetics 1990;63:169–76.

[23] Gligor TD, Manea T, Policec A, Ciocloda G. Electronica medicala. Dacia: Cluj, 1986.

[24] Gillard DM, Prochazka A, Gauthier MJ. Tremor suppression using functional electrical stimulation: a comparison between digital and analog controllers. IEEE Trans Rehabil 1999;Eng.7(3):385–8.

[25] Halliday DM, Conway BA, Farmer SF, Rosenberg JR. Load-independent contributions from motor-unit synchronization to human physiological tremor. J Neurophysiol 1999;82(2):664–75.

[26] Hanna M, Mills K, Pazdera L, Newsom-Davis J. Primary orthostatic tremor with prominent muscle hypertrophy. Neurology 1997;49(3):872–4.

[27] Iokibe T. Fusion of fuzzy and chaos, and its application in industrial field: time series prediction. In: Proceedings of the International Conference on Artificial Neural Networks in Engineering ANNIE'96, 1996; St. Louis, MI, USA.
[28] Jankovic J, Schwartz KS, Ondo W. Re-emergent tremor of Parkinson's disease. J Neurol Neurosurg Psychiatr 1999;67(5):646–50.
[29] Jurgens J, Patterson PE. Development and evaluation of an inexpensive sensor system for use in measuring relative finger positions. Med Eng Phys 1997;19(1):1–6.
[30] Kosanovic BR, Chaparro LF, Sun M, Sclabassi RJ. Signal analysis in fuzzy information space. Fuzzy Sets Syst 1996;77:49–62.
[31] Lakie M, Combes N. There is no simple temporal relationship between the initiation of rapid reactive hand movements and the phase of an enhanced physiological tremor in man. J Physiol London 2000;523(2):515–22.
[32] Lakie M, Combes N. Tremulousness — the perception of tremor in man. Exp Physiol 1999;84(4):807–10.
[33] Lauk M, Timmer J, Honerkamp J, Deuschl G. A software for recording and analysis of human tremor. Comput Methods Programs Biomed 1999;60(1):65–77.
[34] Lemstra AW, Verhagen Metman L, Lee JI, Dougherty PM, Lenz FA. Tremor-frequency (3–6 Hz) activity in the sensorimotor arm representation of the internal segment of the globus pallidus in patients with Parkinson's disease. Neurosci Lett 1999;267(2):129–32.
[35] Lin CD, Zev Rymer W. A quantitative analysis of pendular motion of the lower leg in spastic human subjects. IEEE Trans BME 1991;38(9):906–18.
[36] Liu X, Tubbesing SA, Aziz TZ, Miall RC, Stein JF. Effects of visual feedback on manual tracking and action tremor in Parkinson's disease. Exp Brain Res 1999;129(3):477–81.
[37] Louis ED, Yousefzadeh E, Barnes LF, Yu Q, Pullman SL, Wendt KJ. Validation of a portable instrument for assessing tremor severity in epidemiologic field studies. Mov Disord 2000;15(1):95–102.
[38] Louis ED, Wendt KJ, Albert SM, Pullman SL, Yu Q, Andrews H. Validity of a performance-based test of function in essential tremor. Arch Neurol 1999;56(7):841–6.
[39] Lundervold DA, Belwood MF, Craney JL, Poppen R. Reduction of tremor severity and disability following behavioral relaxation training. J Behav Ther Exp Psychiatr 1999;30(2):119–35.
[40] Meijer GAL, et al. Methods to assess physical activity with special reference to motion sensors and accelerometers. IEEE Trans BME 1991;38(3):221–9.
[41] Micera S, Sabatini AM, Dario P. Adaptive fuzzy control of electrically stimulated muscles for arm movements. Med Biol Eng Comput 1999;37(6):680–5.
[42] Milanov I, Toteva S, Georgiev D. Alcohol withdrawal tremor. Electromyogr Clin Neurophysiol 1996;36(1):15–20.
[43] Morrison S, Newell KM. Postural and resting tremor in the upper limb. Clin Neurophysiol 2000;111(4):651–63.
[44] Norman KE, Edwards R, Beuter A. The measurement of tremor using a velocity transducer: comparison to simultaneous recordings using transducers of displacement acceleration and muscle activity. J Neurosci Methods 1999;92(1/2):41–54.
[45] Raethjen J, Lindemann M, Schmaljohann H, Wenzelburger R, Pfister G, Deuschl G. Multiple oscillators are causing Parkinsonian and essential tremor. Mov Disord 2000;15(1):84–94.
[46] Rajaraman V, Jack D, Adamovich SV, Hening W, Sage J, Poizner H. A novel quantitative method for 3D measurement of Parkinsonian tremor. Clin Neurophysiol 2000;111(2):338–43.
[47] Rodriguez W, Teodorescu HN, Bunke H, Kandel A. A fuzzy information space approach to movement nonlinear analysis. Int J Chaos Theory Appl 1998;3(12):29–38.
[48] Staude G, Wolf W, Ott M, Dengler R. Oertel WH., Tremor as a factor in prolonged reaction times of Parkinsonian patients. Mov Disord 1995;10(2):153–62.
[49] Teodorescu HN. Research Report, Grant 7RUPJ-48689, (1996–1998). Swiss Federal Institute of Technology, and National Swiss Funds, Switzerland, 1998.
[50] Teodorescu HN, Kandel A, Teodorescu C, Mlynek D, Rodriguez W, Posa C, Ropota I. Fuzzy methods of fusing classic and chaotic numerical parameters in a hand tremor rehabilitation system. In: Proceedings of IIZUKA'98 International Conference, 1998 August; Iizuka, Japan.

[51] Teodorescu HN. Position and movement resonant sensor. United States Patent No. 5,986,549 (1999), also Patent RO112918 (1998), Patent Request AU8641498.
[52] Teodorescu HN, Mlynek D. Respiration and movement monitoring system. United States Patent No. 6,011,477 (2000).
[53] Teodorescu HN, Kandel A, Jain LC, editors. Fuzzy and neuro-fuzzy systems in medicine. Boca Raton FL, USA: CRC Press (ISBN0-8493-9806-1), 1998.
[54] Teodorescu HN, Jain LC, editors. Intelligent technologies for rehabilitation. Boca Raton FL, USA: CRC Press (Scheduled summer 2000).
[55] Teodorescu HN, Bonciu C. Feature-oriented hybrid neural adaptive systems and applications. In: Teodorescu HN, Mlynek D, Kandel A, Zimmermann HJ, editors. Intelligent systems and interfaces. The Kluwer International Series in Intelligent Technologies, vol. 15. Boston: Kluwer Academic Publishers.
[56] Teodorescu HN, Kandel A. Nonlinear analysis of limbs and head movements. Jpn J Med Electron Biomed Eng (Japan) 1999;13(5):11–20.
[57] Toth-Cohen S, Petralia PB, Miller KS. Therapists' experiences with computer-assisted instruction in hand therapy. J Hand Ther 1997;10(1):41–5.
[58] Wang LX. Fuzzy systems are universal approximators. In: Proceedings of IEEE International Conference on Fuzzy Systems, San Diego, CA, USA, 1992. p. 1163–70
[59] Wang LX. Adaptive fuzzy systems and control. New York: Prentice-Hall, 1993.
[60] Yamakawa T, et al. A neo-fuzzy neuron and its applications to system identification and prediction of the system behavior. In: Proceedings of International Conference on Fuzzy Logic and Neural Networks, 1992; Iizuka, Japan. p. 477–83.
[61] Zimmermann R, Deuschl G, Hornig A, Schulte-Monting J, Fuchs G, Lucking CH. Tremors in Parkinson's disease: symptom analysis and rating. Clin Neuropharmacol 1994;4:303–14.